JACS
JOURNAL OF THE AMERICAN CHEMICAL SOCIETY

Communication

pubs.acs.org/JACS

Well-Defined Thiolated Nanographene as Hole-Transporting Material for Efficient and Stable Perovskite Solar Cells

Jing Cao,[†,∥] Yu-Min Liu,[†,∥] Xiaojing Jing,[†] Jun Yin,[†,‡] Jing Li,[‡] Bin Xu,[§] Yuan-Zhi Tan,*[,†] and Nanfeng Zheng*[,†]

[†]Collaborative Innovation Center of Chemistry for Energy Materials, State Key Laboratory for Physical Chemistry of Solid Surfaces, Engineering Research Center for Nano-Preparation Technology of Fujian Province, and Department of Chemistry, College of Chemistry and Chemical Engineering, Xiamen University, Xiamen 361005, China

[‡]Pen-Tung Sah Institute of Micro-Nano Science and Technology, Xiamen University, Xiamen 361005, China

[§]State Key Laboratory of Supramolecular Structure and Materials, Jilin University, Changchun 130012, China

Supporting Information

ABSTRACT: Perovskite solar cells (PSCs) have been demonstrated as one of the most promising candidates for solar energy harvesting. Here, for the first time, a functionalized nanographene (perthiolated trisulfur-annulated hexa-*peri*-hexabenzocoronene, TSHBC) is employed as the hole transporting material (HTM) in PSCs to achieve efficient charge extraction from perovskite, yielding the best efficiency of 12.8% in pristine form. The efficiency is readily improved up to 14.0% by doping with graphene sheets into TSHBC to enhance the charge transfer. By the HOMO−LUMO level engineering of TSHBC homologues, we demonstrate that the HOMO levels are critical for the performance of PSCs. Moreover, beneficial from the hydrophobic nature of TSHBC, the devices show the improved stability under AM 1.5 illumination in the humidity about 45% without encapsulation. These findings open the opportunities for efficient HTMs based on the functionalized nanographenes utilizing the strong interactions of their functional groups with perovskite.

The solution-processed hybrid perovskite solar cells (PSCs) have drawn dramatically increased attentions as a real competitor to silicon solar cell,[1−10] due to their high power conversion efficiencies, easy fabrication, and low-cost. Clearly, a large amount of the converted photon energy is wasted by the surface recombination resulting from the imperfect crystal passivation and undesirable interfacial behavior. Therefore, further efficiency enhancement mainly relies on minimizing the interface losses by interface modification between the active layers.[11−13] More recent studies have revealed that the interfacial modification between perovskite and electron collecting layers can enhance the efficiencies of PSCs,[12−15] while the hole transporting materials (HTM) at the other side of perovskite layer also play an important role in the most efficient PSCs. An ideal HTM generally requires compatible energy level and sufficient charge extraction and transferability.[3−8,16−18] Carbon materials with unique conductivity properties, such as porous carbon,[9,12] graphene,[19] graphdiyne,[20] graphene oxide,[21] and single-walled carbon nanotube,[22] have been successfully utilized as hole extraction and transfer materials in PSCs.

Nanographenes are nanosized graphene molecules with defined chemical structures.[23] Their physical and chemical nature is essentially determined by their size and peripheral structure.[24,25] In past decades, nanographenes have been intensively investigated as organic semiconductors due to its excellent self-assembly properties and large conjugated π system.[26] In general, nanographenes are typical *p*-type semiconductors,[26,27] and their electronic properties such as HOMO−LUMO energy level, electron-donating ability, and processability are ready to be modulated by rational functionalization,[28,29] which render nanographenes promising candidates for the HTMs of PSCs. However, to the best of our knowledge, none of the nanographenes has been employed in PSCs as HTMs to date. Meanwhile, the functional groups at the periphery of nanographenes provide the possibility to tune the interactions (such as coordination interactions) with perovskite layer in PSCs, which would facilitate the charge extraction and transport from perovskite to nanographenes; therewith improving the efficiencies of PSCs but was rarely studied at current stage.

Here we use a thiolated nanographene perthiolated trisulfur-annulated hexa-*peri*-hexabenzocoronene (TSHBC, the structure shown in Figure 1a) as the HTM in the pristine form in PSCs. The thiol groups at the periphery form Pb−S coordination-bonds at the interface of perovskite and HTM. The tight binding of TSHBC helps to rapidly extract charge from perovskite, resulting in a low energy loss at the interface. The performance is readily improved by doping with graphene sheets into TSHBC to enhance the hole transporting property within HTM. By tuning the HOMO level of TSHBCs, the HOMO level of HTMs is revealed as a key issue for the performance of HTMs in PSCs. Moreover, the long-term stability is the biggest remaining challenging issue for the commercialization of PSCs. In order to resolve this issue, various strategies have been proposed and investigated.[9,22,30−33] Hydrophobic thiolated nanographenes reported in this work would provide as an effective molecular sealing approach to improve the stability of PSCs.

TSHBC was synthesized following a recently reported method (see Supporting Information for details)[34] and used as HTM for the fabrication of PSCs. The fabricated PSCs had a typical p-i-n

Received: June 23, 2015
Published: August 18, 2015

DOI: 10.1021/jacs.5b06493
J. Am. Chem. Soc. 2015, 137, 10914−10917

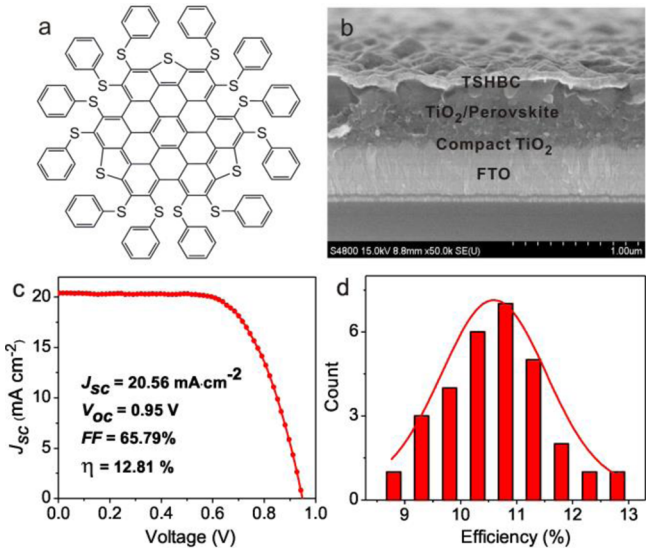

Figure 1. (a) Structures of TSHBC. (b) Cross-sectional SEM image of the device of FTO/TiO_2/perovskite/TSHBC film. (c) Best I–V characteristics. (d) Comparison of the performance distributions of 30 individual devices of the cells.

configuration of FTO/TiO_2/$CH_3NH_3PbI_3$/TSHBC. In a typical fabrication procedure, the compact TiO_2 layer and mesoporous TiO_2 layer were deposited on a FTO (fluorine doped tin oxide) conducting glass substrate, to achieve electron extraction and transport. Contrary to the conventional PSCs using spiro-OMeTAD as HTM, we employed here TSHBC (20 nm thickness) on top of perovskite layer as HTM. The entire fabrication procedure was completed in the open air at a common relative humidity of 45%. The fabricated perovskite devices were characterized by SEM (Figure 1b), UV–vis (Figure S1), and XRD (Figure S2).

To evaluate whether TSHBC could serve as an effective material to extract photogenerated holes from the perovskite layer, the J–V characteristics of FTO/TiO_2/$CH_3NH_3PbI_3$/TSHBC device were measured under the illumination of AM 1.5, 100 mW cm^{-2}. As shown in Figure 1c, when ~20 nm thick TSHBC was deposited on the top of the perovskite layer as HTM, the best efficiency of 12.8% was successfully achieved. The open-circuit voltage (V_{oc}), short-cut current (J_{sc}), and fill-factor (FF) of the cell were measured to be 0.95 V, 20.56 mA·cm^{-2}, and 65.79%, respectively. The measurements over 30 fabricated devices gave an average efficiency of 10.6 ± 2.2% (Figure 1d).The incident photon-to-current conversion efficiency spectra (IPCE) of the device spanned from the UV region to 800 nm (Figure S3), matching well with its UV–vis absorption spectra (Figure S1).

The excellent performance of PSCs involving the use of TSHBC as HTM suggested a unique hole-extracting interface between perovskite and TSHBC. Infrared (IR) spectra of the films during the fabrication of devices were thus measured to evaluate the interactions between perovskite and TSHBC. In the IR spectrum of the TiO_2/perovskite/TSHBC film (Figure S4), there was an appearance of absorption peak at 432 cm^{-1} that was assigned to Pb–S vibration,[15] and the C–S absorption peak at 700 cm^{-1} became weaker and slightly blue-shifted compared to that of pure TSHBC. These results clearly suggested the formation of Pb–S coordination-bond between TSHBC and perovskite. We propose that the formation of Pb–S coordination-bond between TSHBC and perovskite contributes the efficient electron extraction at the interface.

In order to have photogenerated holes effectively extracted into HTM, the matching of HOMO level of HTM with the valence-band level of perovskite should be a critical factor. The easy chemical modification of TSHBCs allows us to verify this hypothesis experimentally. By decorating electron-donating or with drawing groups at the periphery of TSHBC, the HOMO–LUMO levels of TSHBC homologues can be reasonably modulated without changing other properties, making it possible to investigate the impact of the HTM's HOMO level on the efficiencies of PSCs. Two TSHBC homologues (TSHBC–tBu and TSHBC–CF_3) bearing 12 4-t-butylphenyl groups and 4-trifluoromethylphenyl groups at the periphery were synthesized. The HOMO–LUMO energy levels of TSHBC homologues were obtained by the cyclic voltammetric measurements under the same condition with ferrocene as an internal standard (Figure S5 and Table S1). As shown in Figure 2a, the HOMO levels of TSHBC–tBu and TSHBC–CF_3 were measured to be −5.27 and −5.70 eV, 0.13 eV higher and 0.3 eV lower than that of TSHBC, respectively.

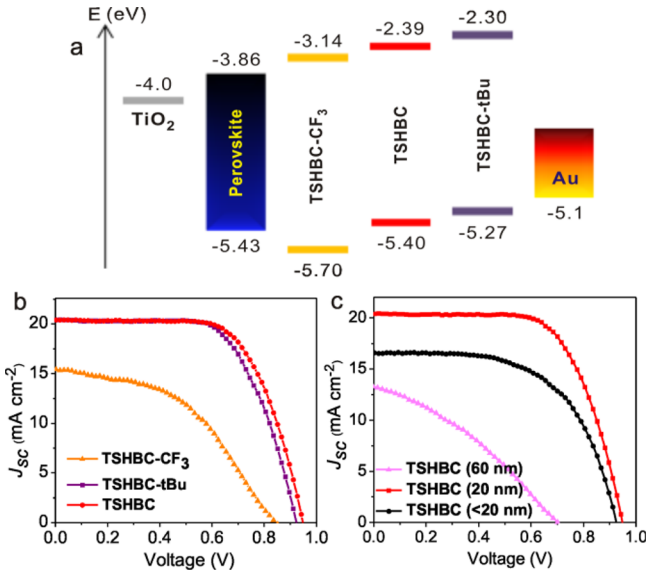

Figure 2. (a) Energy level diagram of the materials used in PSCs. (b) Best I–V characteristics of the cells. (c) Best I–V characteristics of the cells based on TSHBC with different thickness.

The variation in the energy levels is expected to impact the performances of PSCs using TSHBC–tBu and TSHBC–CF_3 as HTMs. The PSCs devices with 20 nm TSHBC–tBu and TSHBC–CF_3 layers were fabricated, and their PCEs were measured. As illustrated in Figures 2b, S6, and S7, the devices based on TSHBC–tBu offered an average efficiency of 9.9 ± 2.3% with the best efficiency of 12.2%. In comparison with devices based on TSHBC, TSHBC–tBu based devices had a similar J_{sc}, but a slightly lower V_{oc}. The lower V_{oc} is attributed to the higher HOMO level of TSHBC–tBu than that of TSHBC. In remarkable contrast, the TSHBC–CF_3-based devices showed a much poorer photovoltaic performance with the best efficiency of 6.1% (the average efficiency of 4.5 ± 2.7%). This value was even lower than that of the devices with no HTM (Figure S7 and Table S2), indicating that TSHBC–CF_3 hindered the hole transfer from perovskite due its lower HOMO level than the top of valence band of perovskite. The longer PL decay time of the

DOI: 10.1021/jacs.5b06493
J. Am. Chem. Soc. 2015, 137, 10914–10917

film with TSHBC−CF_3 (Figure S8) also suggested the similar result. These results from three different TSHBC homologues clearly demonstrate that, in order to maximize the overall performance of PSCs, the HOMO level of HTMs should be higher than but close enough to the top of valence band of perovskite.

With 12 phenylthio groups decorated at their periphery, TSHBC and its homologues are not strictly planar and thus not expected to serve as an excellent hole transporting material. Indeed, space-charge-limited current measurement revealed negligible hole transport mobility ($\mu = 4.0 \times 10^{-15}$ $cm^2 \cdot V^{-1} \cdot s^{-1}$) for TSHBC (Figure S9).[35] Similarly, both TSHBC−*t*Bu and TSHBC−CF_3 also exhibited poor hole transporting properties (Table S1). Considering the poor hole transporting property of TSHBC and its homologues is deleterious to the overall performance of PSCs, one can suppose that a thicker film of TSHBC in the device would lead to a poorer performance. As expected, a much poorer performance was observed on the devices with thicker (60 nm) TSHBC layers (Figures 2c and S10 and Table S3). The best performance of the cells was only 3.2%. In contrast, the PCEs should be improved by decreasing the thickness of TSHBC layer. Unfortunately, due to the high roughness of pervoskite layer, when the thickness of TSHBC in the device was further decreased below 20 nm, a lot of pinholes were present in the TSHBC layer (Figure S10b). Consequently, the fabricated PSCs showed an overall performance similar to that of devices with no HTM layer (Figure S11 and Table S3).

To further understand the impact of thickness of TSHBC on the cells' performances, electrochemical impedance spectra (EIS) of PSCs with TSHBC of various thicknesses were measured in the dark condition. At the 0.8 mV forward bias voltage, the greatly increased charge-transport resistance, obtained from the semicircles at high-intermediate frequency,[36,37] was observed as the thickness of HTM increased from 20 to 60 nm (Figure S12). The increased resistance could be ascribed to the disadvantageous charge transfer within the thicker HTM layer,[3] in good agreement with the *J*−*V* characteristics above-mentioned.

HTM in PSCs usually plays both roles to extract holes from perovskite and transport holes to the current collecting electrode. The results discussed above have demonstrated that TSHBC molecules readily achieve effective hole extraction from perovskite. However, their poor hole transporting behavior would be a limiting factor to further improve the performance of PSCs. To resolve this issue, highly conductive graphene sheets were incorporated into the TSHBC layer (Figure S13). When the thickness was 20 nm for the HTM layer, the ratio of graphene and TSHBC was optimized (Figure S14 and Table S4). For the devices base on the optimized TSHBC/graphene (5:1, weight ratio), the significantly enhanced performance with the best efficiency of 14.0% (Figure 3a) was observed. Both V_{oc} and J_{sc} were improved. The measurements over 30 fabricated devices gave an average efficiency of 12.0 ± 2.1% (Figure S7). This result demonstrated the introduction of highly conductive materials helped to improve the hole transporting property of TSHBC and thus enhanced overall photovoltaic performance of PSCs. However, it should be noted that the presence of photocurrent hysteresis was revealed in both cells with TSHBC and TSHBC/graphene as HTMs (Figure S15 and Table S5), which could be due to the nature of the perovskite films.

In order to further verify the improved hole transfer within the TSHBC/graphene layer, the transient photoluminescence (PL) spectra were measured. As illuminated in Figure 3b, compared to

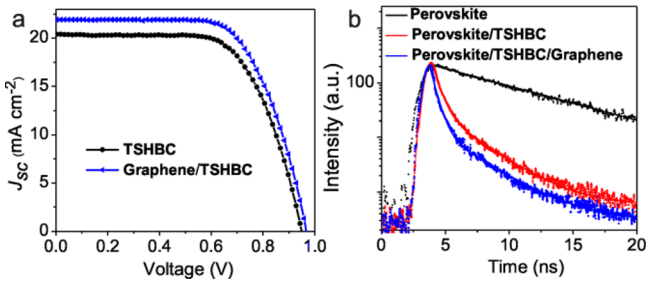

Figure 3. Best *I*−*V* characteristics of the cells (a) and transient PL spectra of films (b), based on 20 nm HTM layers.

the perovskite-only film with a decay time (τ) of 73.6 ns, the introduction of TSHBC on the top of the perovskite layer shortened the PL decay time to 6.1 ns. Furthermore, the film with perovskite-TSHBC/graphene displayed a shorter PL decay time of 3.5 ns. The quenched photoinduced excitons at the pervoskite/HTMs interface clearly confirmed that introducing graphene enhanced the hole transporting property of TSHBC as HTM.

Another important advantage of thiolated nanographenes as HTM lies in their hydrophobicity, which is readily provided as an effective molecular sealing approach to improve the stability of PSCs. In our previous work,[15] we found that the hydrophobic thiols on perovskite surface readily inhibited the entrance of water molecules into perovskite film to significantly enhance the stability of PSCs. As shown in Figures 4a and S16, the contact

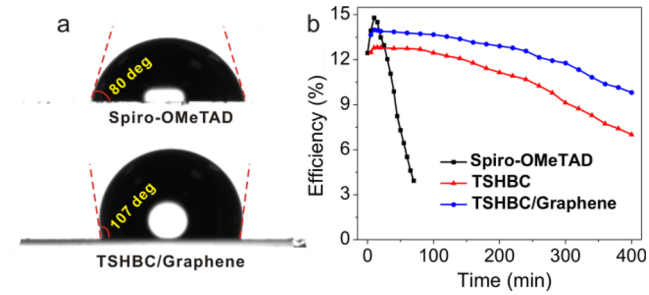

Figure 4. (a) Water contact angles. (b) Efficiency variation of the devices stored under illumination at AM 1.5 G with the humidity of 45%.

angles of water droplets on both TSHBC and TSHBC/graphene were ~107°, while the angle was only 70° on spiro-OMeTAD. The excellent hydrophobic properties of thiolated TSHBC and TSHBC/graphene should improve the long-term durability of the devices. In this work, the stabilities of the devices with 20 nm TSHBC and TSHBC/graphene layers were measured under AM 1.5 illumination in the humidity about 45% without any encapsulation. When stored in air with a relative humidity of ~45% (Figure S17), the devices with TSHBC retained over 85% of their original efficiency after 10 days, while the cell based on TSHBC/graphene kept more than 90% of its original efficiency. In contrast, under the same storage condition, the cells with spiro-OMeTAD lost ~80% of their efficiency after 10 days. As shown in Figure 4b, the efficiency of devices with spiro-OMeTAD was decreased to 25% within 60 min under illumination at AM 1.5 G. However, under the same illumination condition for 400 min, the device with TSHBC retained over 60% of its original efficiency, and the cell with TSHBC/graphene still kept more than 70% of its original efficiency. The rapid decrease of the efficiency can be described to accelerating

DOI: 10.1021/jacs.5b06493
J. Am. Chem. Soc. 2015, 137, 10914−10917

decomposition effects from intrinsic thermal instability during illumination, consistent with the reported result.[38]

In summary, thiolated nanographene molecules have been successfully demonstrated as a new type of hole transporting material for fabricating high-performance PSCs. The best efficiency of 12.8% was achieved by using TSHBC as HTM. The energy level matching between the HOMO of TSHBC and valence band of perovskite was critical to the overall performance of PSCs. Detailed studies revealed that the TSHBC layer had rather poor charge transfer characteristics. The further improved overall efficiency of PSCs up to 14% was readily achieved by doping the HTM layer of TSHBC with graphene to enhance the efficient hole transport. More importantly, due to the hydrophobic nature of TSHBC, the devices involving TSHBC exhibited significantly improved device stability. All these findings validate nanographenes as a promising HTM for PSCs. However, the poor hole mobility of these nanographene molecules is one important factor to limit the fill-factor and thus overall efficiency of perovskite solar cells based on them. The performance of nanographenes as HTMs in PSCs can be further improved in terms of edge functionalization and core−structure modulation. This work also suggests the possibility to use functional graphene materials, for example, the thiolated graphene nanoribbons and thiolated graphene sheets, as the HTMs in PSCs.

■ ASSOCIATED CONTENT

Supporting Information

The Supporting Information is available free of charge on the ACS Publications website at DOI: 10.1021/jacs.5b06493.

Experimental details, details of the XRD, UV−vis spectra, cross-sectional SEM images, and the transient PL spectra of the cells based on different TSHBC homologues (PDF)

■ AUTHOR INFORMATION

Corresponding Authors

*nfzheng@xmu.edu.cn

*yuanzhi_tan@xmu.edu.cn

Author Contributions

‖J.C. and Y.-M.L. contributed equally to this work.

Notes

The authors declare no competing financial interest.

■ ACKNOWLEDGMENTS

We thank the MOST of China (2011CB932403) and the NSFC of China (21420102001, 21131005, 21390390, 21333008, and 21401156) for financial support.

■ REFERENCES

(1) Kojima, A.; Teshima, K.; Shirai, Y.; Miyasaka, T. *J. Am. Chem. Soc.* **2009**, *131*, 6050.

(2) Im, J. H.; Lee, C. R.; Lee, J. W.; Park, S. W.; Park, N. G. *Nanoscale* **2011**, *3*, 4088.

(3) Kim, H. S.; Lee, C. R.; Im, J. H.; Lee, K. B.; Moehl, T.; Marchioro, A.; Moon, S. J.; Humphry-Baker, R.; Yum, J. H.; Moser, J. E.; Gratzel, M.; Park, N. G. *Sci. Rep.* **2012**, *2*, 1.

(4) Lee, M. M.; Teuscher, J.; Miyasaka, T.; Murakami, T. N.; Snaith, H. J. *Science* **2012**, *338*, 643.

(5) Liu, M.; Johnston, M. B.; Snaith, H. J. *Nature* **2013**, *501*, 395.

(6) Zhou, H.; Chen, Q.; Li, G.; Luo, S.; Song, T. B.; Duan, H. S.; Hong, Z.; You, J.; Liu, Y.; Yang, Y. *Science* **2014**, *345*, 542.

(7) Jeon, N. J.; Noh, J. H.; Yang, W. S.; Kim, Y. C.; Ryu, S.; Seo, J.; Seok, S. I. *Nature* **2015**, *517*, 476.

(8) Yang, W. S.; Noh, J. H.; Jeon, N. J.; Kim, Y. C.; Ryu, S.; Seo, J.; Seok, S. I. *Science* **2015**, *348*, 1234.

(9) Mei, A.; Li, X.; Liu, L.; Ku, Z.; Liu, T.; Rong, Y.; Xu, M.; Hu, M.; Chen, J.; Yang, Y.; Grätzel, M.; Han, H. *Science* **2014**, *345*, 295.

(10) Nie, W.; Tsai, H.; Asadpour, R.; Blancon, J.-C.; Neukirch, A. J.; Gupta, G.; Crochet, J. J.; Chhowalla, M.; Tretiak, S.; Alam, M. A.; Wang, H.-L.; Mohite, A. D. *Science* **2015**, *347*, 522.

(11) Min, J.; Zhang, Z.-G.; Hou, Y.; Ramirez Quiroz, C. O.; Przybilla, T.; Bronnbauer, C.; Guo, F.; Forberich, K.; Azimi, H.; Ameri, T.; Spiecker, E.; Li, Y.; Brabec, C. J. *Chem. Mater.* **2015**, *27*, 227.

(12) Liu, L.; Mei, A.; Liu, T.; Jiang, P.; Sheng, Y.; Zhang, L.; Han, H. *J. Am. Chem. Soc.* **2015**, *137*, 1790.

(13) Zuo, L.; Gu, Z.; Ye, T.; Fu, W.; Wu, G.; Li, H.; Chen, H. *J. Am. Chem. Soc.* **2015**, *137*, 2674.

(14) Ogomi, Y.; Morita, A.; Tsukamoto, S.; Saitho, T.; Shen, Q.; Toyoda, T.; Yoshino, K.; Pandey, S. S.; Ma, T.; Hayase, S. *J. Phys. Chem. C* **2014**, *118*, 16651.

(15) Cao, J.; Yin, J.; Yuan, S.; Zhao, Y.; Li, J.; Zheng, N. *Nanoscale* **2015**, *7*, 9443.

(16) Lv, S.; Han, L.; Xiao, J.; Zhu, L.; Shi, J.; Wei, H.; Xu, Y.; Dong, J.; Xu, X.; Li, D.; Wang, S.; Luo, Y.; Meng, Q.; Li, X. *Chem. Commun.* **2014**, *50*, 6931.

(17) Heo, J. H.; Song, D. H.; Han, H. J.; Kim, S. Y.; Kim, J. H.; Kim, D.; Shin, H. W.; Ahn, T. K.; Wolf, C.; Lee, T. W.; Im, S. H. *Adv. Mater.* **2015**, *27*, 3424.

(18) Yu, Z.; Sun, L. *Adv. Energy Mater.* **2015**, *5*, 201500213.

(19) Yan, K.; Wei, Z.; Li, J.; Chen, H.; Yi, Y.; Zheng, X.; Long, X.; Wang, Z.; Wang, J.; Xu, J.; Yang, S. *Small* **2015**, *11*, 2269.

(20) Xiao, J.; Shi, J.; Liu, H.; Xu, Y.; Lv, S.; Luo, Y.; Li, D.; Meng, Q.; Li, Y. *Adv. Energy Mater.* **2015**, *5*, 201401943.

(21) Wu, Z.; Bai, S.; Xiang, J.; Yuan, Z.; Yang, Y.; Cui, W.; Gao, X.; Liu, Z.; Jin, Y.; Sun, B. *Nanoscale* **2014**, *6*, 10505.

(22) Habisreutinger, S. N.; Leijtens, T.; Eperon, G. E.; Stranks, S. D.; Nicholas, R. J.; Snaith, H. J. *Nano Lett.* **2014**, *14*, 5561.

(23) Müllen, K. *ACS Nano* **2014**, *8*, 6531.

(24) Yan, L.; Zheng, Y. B.; Zhao, F.; Li, S.; Gao, X.; Xu, B.; Weiss, P. S.; Zhao, Y. *Chem. Soc. Rev.* **2012**, *41*, 97.

(25) Fujii, S.; Enoki, T. *Acc. Chem. Res.* **2013**, *46*, 2202.

(26) Wu, J.; Pisula, W.; Muellen, K. *Chem. Rev.* **2007**, *107*, 718.

(27) Feng, X.; Marcon, V.; Pisula, W.; Hansen, M. R.; Kirkpatrick, J.; Grozema, F.; Andrienko, D.; Kremer, K.; Mullen, K. *Nat. Mater.* **2009**, *8*, 421.

(28) Kumar, S. *Chem. Soc. Rev.* **2006**, *35*, 83.

(29) Sergeyev, S.; Pisula, W.; Geerts, Y. H. *Chem. Soc. Rev.* **2007**, *36*, 1902.

(30) Liu, J.; Wu, Y.; Qin, C.; Yang, X.; Yasuda, T.; Islam, A.; Zhang, K.; Peng, W.; Chen, W.; Han, L. *Energy Environ. Sci.* **2014**, *7*, 2963.

(31) Shi, D.; Adinolfi, V.; Comin, R.; Yuan, M.; Alarousu, E.; Buin, A.; Chen, Y.; Hoogland, S.; Rothenberger, A.; Katsiev, K.; Losovyj, Y.; Zhang, X.; Dowben, P. A.; Mohammed, O. F.; Sargent, E. H.; Bakr, O. M. *Science* **2015**, *347*, 519.

(32) Smith, I. C.; Hoke, E. T.; Solis-Ibarra, D.; McGehee, M. D.; Karunadasa, H. I. *Angew. Chem., Int. Ed.* **2014**, *53*, 11232.

(33) Jiang, Q.; Rebollar, D.; Gong, J.; Piacentino, E. L.; Zheng, C.; Xu, T. *Angew. Chem., Int. Ed.* **2015**, *54*, 7617.

(34) Tan, Y. Z.; Osella, S.; Liu, Y.; Yang, B.; Beljonne, D.; Feng, X.; Mullen, K. *Angew. Chem., Int. Ed.* **2015**, *54*, 2927.

(35) Mihailetchi, V. D.; Xie, H. X.; de Boer, B.; Koster, L. J. A.; Blom, P. W. M. *Adv. Funct. Mater.* **2006**, *16*, 699.

(36) Kim, H. S.; Mora-Sero, I.; Gonzalez-Pedro, V.; Fabregat-Santiago, F.; Juarez-Perez, E. J.; Park, N. G.; Bisquert, J. *Nat. Commun.* **2013**, *4*, 2242.

(37) Xu, X.; Liu, Z.; Zuo, Z.; Zhang, M.; Zhao, Z.; Shen, Y.; Zhou, H.; Chen, Q.; Yang, Y.; Wang, M. *Nano Lett.* **2015**, *15*, 2402.

(38) Conings, B.; Drijkoningen, J.; Gauquelin, N.; Babayigit, A.; D'Haen, J.; D'Olieslaeger, L.; Ethirajan, A.; Verbeeck, J.; Manca, J.; Mosconi, E.; Angelis, F. D.; Boyen, H.-G. *Adv. Energy Mater.* **2015**, *5*, 201500477.

DOI: 10.1021/jacs.5b06493
J. Am. Chem. Soc. 2015, 137, 10914−10917